Thermochimica Acta, 173 (1990) 53–62
Elsevier Science Publishers B.V., Amsterdam

KINETIC STUDY OF THE THERMAL DEHYDRATION OF COPPER(II) ACETATE MONOHYDRATE. II. CRUSHED CRYSTALS

HARUHIKO TANAKA * and NOBUYOSHI KOGA

Chemistry Laboratory, Faculty of School Education, Hiroshima University, Shinonome, Minami-ku, Hiroshima 734 (Japan)

(Received 2 April 1990)

ABSTRACT

Kinetic analysis of the thermal dehydration of crushed crystals of $Cu(CH_3COO)_2 \cdot H_2O$ was made by use of TG and DSC curves recorded under comparable experimental conditions. Isothermal TG was also employed, and the result was compared with that obtained nonisothermally. The isothermal reaction was described by a phase-boundary controlled reaction (R_n) law, $1-(1-\alpha)^{1/n} = kt$, with $1 < n < 2$. As for the nonisothermal reaction, there was a tendency for the appropriate kinetic law determined from TG to change from an Avrami–Erofeyev (A_m) law, $[-\ln(1-\alpha)]^{1/m} = kt$, to one of diffusion-controlled reaction (D_L) laws as the reaction advanced, particularly for a larger particle-size fraction of the sample. According to DSC, the nonisothermal kinetics were described exclusively by an A_m law. The difference in kinetics determined from TG and DSC was explained by the nature of the two methods.

INTRODUCTION

Recently we have shown that dehydration of the single crystal of copper(II) acetate monohydrate proceeds through advancement of the reaction front [1]. Kinetic obedience of the isothermal dehydration was described by a phase-boundary controlled reaction (R_n) law, $1-(1-\alpha)^{1/n} = kt$, with $2 < n < 3$. On the other hand, the nonisothermal dehydration of the single crystal followed a diffusion-controlled reaction (D_4) law, $1-2\alpha/3-(1-\alpha)^{2/3} = kt$, particularly at higher heating rates and at later stages of the reaction.

As an extension of the above kinetic study, it is worth investigating the kinetics of dehydration of the crushed crystals of various particle-size fractions, in that the kinetics of solid-state reactions are in general largely influenced by the sample condition. In particular, it is interesting to follow the nonisothermal kinetics more comprehensively because kinetic obedience might differ between the single crystal and crushed crystals, as well as

* Author to whom correspondence should be addressed.

0040-6031/90/$03.50

among different particle-size fractions of the crushed crystals. In addition, it is likely that a kinetic comparison between the nonisothermal TG and DSC measurements will be useful for assessing the role of a diffusion process during the reaction [2].

Accordingly, nonisothermal TG and DSC measurements, as well as isothermal TG measurements, were undertaken to increase understanding of the kinetics of the reaction. It was hoped that theoretical considerations on kinetics of a given solid-state reaction would be consistent with evidence from such different experimental approaches.

EXPERIMENTAL

Single crystals of the title compound were grown at 45 °C from aqueous solution to which a small amount of acetic acid was added. The crystals were crushed with a mortar and pestle and sieved to different particle-size fractions. The samples were identified by means of IR and TG measurements.

Isothermal mass-change measurements at various constant temperatures from 79 to 110 °C were made on a Shimadzu TGA-50 in a flow of nitrogen at a rate of 30 ml min^{-1}, using 17.0 mg of sample in a platinum crucible (diameter 5 mm and height 2.5 mm). Nonisothermal TG measurements were made at heating rates of 0.4–6.0 K min^{-1} using a Rigaku Thermoflex TG-DSC 8085E1 system under conditions otherwise identical with those for the isothermal runs. The dynamic TG measurements were accompanied by DSC to maintain a linear increase of the sample temperature during the course of reaction by diminishing the self-cooling effect [3]. Under the experimental conditions comparable with those for the nonisothermal TG measurements, DSC curves were also recorded using a Rigaku Thermoflex DSC CN8059L1 system. All the thermoanalytical data were stored in a microcomputer and analyzed kinetically.

RESULTS AND DISCUSSION

Isothermal gravimetry

Figure 1 shows typical plots of fractional reaction, α, against time, t, obtained from mass-loss curves for the isothermal dehydration of powdered $Cu(CH_3COO)_2 \cdot H_2O$ of various particle-size fractions at similar temperatures. Figure 2 shows the typical temperature dependence of α vs. t plots for the isothermal dehydration of the sample of a $-100 + 170$ mesh sieve fraction.

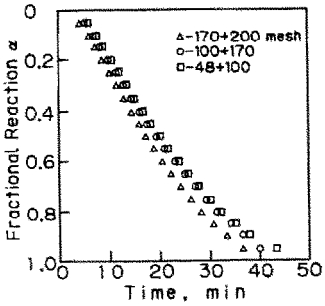

Fig. 1. Typical plots of α against t for the isothermal dehydration of $Cu(CH_3COO)_2 \cdot H_2O$ at ca. 105° C.

Kinetic obedience was determined through plots of various kinetic model functions $F(\alpha)$ against t, assuming the following kinetic equation:

$$F(\alpha) = kt \tag{1}$$

Either a contracting geometry (R_n) law, $1-(1-\alpha)^{1/n} = kt$ with $1 \leqq n \leqq 2$, or an Avrami–Erofeyev (A_m) law, $[-\ln(1-\alpha)]^{1/m} = kt$ with $m \approx 2$, obeyed the isothermal reaction. Table 1 shows the most appropriate $F(\alpha)$ determined by scanning the values of n and m in the R_n and A_m laws, respectively, together with the Arrhenius parameters calculated from the Arrhenius equation for the isothermal dehydration of the crushed crystals of different particle-size fractions. We see from Table 1 that the R_n law with $n \approx 1.4$ gives the best linearity for all the particle-size fractions examined, although obedience to A_m laws is not markedly inferior. It is noted that the kinetic obedience as well as the activation energy (E) value for the largest particle-size fraction ($-48+100$ mesh) compare with those for the single crystal material [1]. In spite of the increase in reaction rate with decrease in particle-size fraction (see Fig. 1), the Arrhenius parameters obtained do not necessarily decrease in line with particle-size fraction. The rate constants, k,

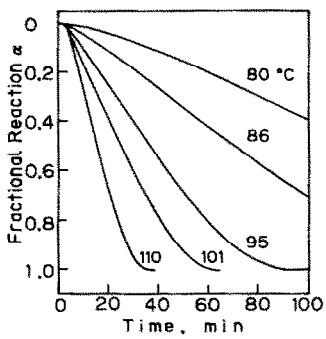

Fig. 2. Typical temperature dependence of α vs. t plots for the isothermal dehydration of $Cu(CH_3COO)_2 \cdot H_2O$, $-100+170$ mesh sieve fraction.

TABLE 1

The most appropriate kinetic rate function, $F(\alpha)$, and Arrhenius parameters obtained from conventional analysis for the isothermal dehydration of the crushed crystals of different particle-size fractions within a range of $0.1 \leqq \alpha \leqq 0.9$

Particle-size fraction, mesh	$F(\alpha)$ [a]	r [b]	E(kJ mol^{-1})	log A (s^{-1})	$-r$ [c]	$k \times 10^4$ (s^{-1}) [d]
−170+200	$R_{1.46 \pm 0.03}$	0.9998	86.2±1.5	8.6±0.2	0.9996	2.26
	$A_{2.10 \pm 0.04}$	0.9990	86.1±1.5	8.7±0.2	0.9996	3.33
−100+170	$R_{1.37 \pm 0.01}$	0.9999	84.6±1.1	8.3±0.2	0.9992	2.08
	$A_{2.19 \pm 0.02}$	0.9989	84.5±1.1	8.5±0.2	0.9991	2.93
−48+100	$R_{1.44 \pm 0.02}$	0.9999	89.5±2.2	9.0±0.3	0.9988	1.89
	$A_{2.09 \pm 0.03}$	0.9991	89.5±2.2	9.2±0.3	0.9987	2.83

[a] $R_n = 1-(1-\alpha)^{1/n}$; $A_m = [-\ln(1-\alpha)]^{1/m}$.
[b] Correlation coefficient of the linear regression analysis of the $F(\alpha)$ vs. t plot.
[c] Correlation coefficient of the linear regression analysis of the Arrhenius plot.
[d] Rate constant at 95°C.

at a given temperature are also listed in Table 1. It is seen that the value of k decreases with increasing particle-size fraction, which confirms the obedience to the R_n law.

The activation energy E at various α values was also obtained by using the following equation, which is derived from eqn. (1) and the Arrhenius equation

$$-\ln t = -E/RT + \ln[A/F(\alpha)] \tag{2}$$

Figure 3 shows such apparent values of E at various α from 0.05 to 0.95 in steps of 0.05 for the isothermal dehydration of the crushed crystals of different particle-size fractions. During the initial reaction ($\alpha \leqq 0.2$), the value of E increases drastically as reaction advances. On the other hand, nearly constant values of E are obtained for the subsequent stages. The variation in the E value in the early stage is likely to arise from surface nucleation and its growth. The main and later stages of the reaction can be

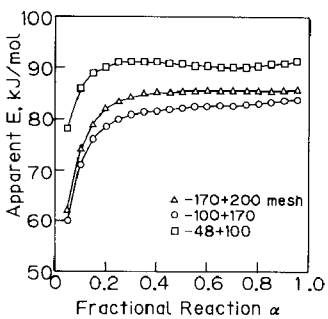

Fig. 3. E values at various values of α for the isothermal dehydration of $Cu(CH_3COO)_2 \cdot H_2O$.

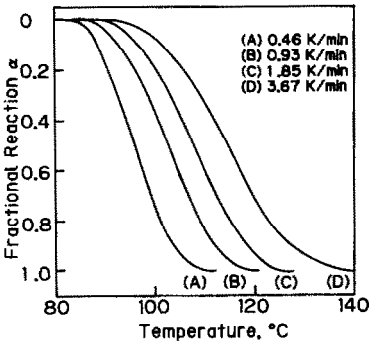

Fig. 4. Typical plots of α vs. T for the nonisothermal dehydration of $Cu(CH_3COO)_2 \cdot H_2O$ at different heating rates.

described by advancement of the reaction interface inwards, because the E values during these stages are consistent with those obtained by the Arrhenius plot (see Table 1).

Nonisothermal analysis

1. TG

Figure 4 shows typical TG curves for the dehydration of the powdered sample at various heating rates. The nonisothermal dehydration of powdered samples was analyzed according to the Ozawa method [4–6] because this is useful particularly for determining kinetic obedience of the nonisothermal reaction [7]. The equations used are the following

$$\ln(\beta/T^2) \approx -E/RT + \ln(R/\theta E) \tag{3}$$

$$\theta \approx (RT^2/\beta E)\exp(-E/RT) \tag{4}$$

$$F(\alpha) = A\theta \tag{5}$$

where θ is the reduced time or generalized time [6]. Figure 5 shows the values of E obtained by assuming eqn. (3) at various α values from 0.10 to

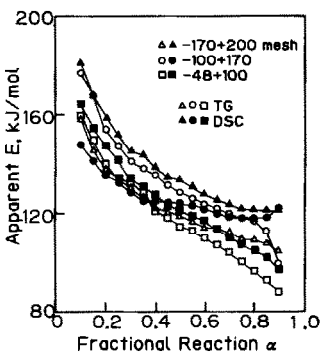

Fig. 5. E values calculated by the Ozawa method at various values of α.

TABLE 2

The most appropriate kinetic rate function, $F(\alpha)$, and Arrhenius parameters, E and log A, determined by the Ozawa method from the TG curves of the nonisothermal dehydration of crushed crystals of different particle-size fractions within various α ranges

Range of α	Particle-size fraction (mesh)											
	−170+200				−100+170				−48+100			
	$F(\alpha)$	E(kJ mol^{-1})	log A(s^{-1})	r [a]	$F(\alpha)$	E(kJ mol^{-1})	log A (s^{-1})	r [a]	$F(\alpha)$	E(kJ mol^{-1})	log A (s^{-1})	r [a]
0.1–0.9	$A_{1.2}$	123±3	14.2±0.4	0.9998	$A_{1.1}$	133±4	13.6±0.4	0.9992	D_2	118±4	13.0±0.2	0.9990
0.1–0.5	$A_{3.0}$	133±3	15.7±0.4	0.9999	$A_{1.0}$	146+4	16.0±0.5	0.9971	$A_{1.0}$	133±4	15.6±0.3	0.9991
0.2–0.6	$A_{1.1}$	125±2	14.5±0.4	0.9999	$A_{1.0}$	136±3	14.5±0.4	0.9979	D_1	124±3	14.0±0.2	0.9995
0.3–0.7	$A_{1.2}$	120±2	13.8±0.5	0.9999	$A_{1.2}$	129±2	13.2±0.4	0.9994	D_2	117±3	12.8±0.3	0.9997
0.4–0.8	$A_{1.1}$	116±2	13.3±0.4	0.9999	$A_{1.0}$	124±2	14.5±0.5	0.9994	D_3	110±2	11.4±0.2	0.9996
0.5–0.9	D_2	112±1	12.7±0.4	0.9997	D_2	118±2	13.2±0.4	0.9989	D_4	103±2	10.4±0.2	0.9996

[a] Correlation coefficient of the linear regression analysis of the $F(\alpha)$ vs. θ plot.

0.90 in steps of 0.05. It is seen that E decreases with increasing α, particularly at smaller α, which is in marked contrast to the findings in isothermal analysis. The variation in E suggests a possible change in kinetic obedience during the course of reaction. θ was recalculated, by using the mean value of E within various restricted ranges of α, according to eqn. (4). Kinetic obedience and pre-exponential factors, A, were determined through plots of various $F(\alpha)$ against θ according to eqn. (5). It should be noted here that the variation in E depending on α is in contradiction to the prerequisite for use of this method. It is interesting, however, to determine kinetic obedience and the A value within various restricted ranges of α, in which the variation in E is smaller, in an attempt to detect any possible change in rate behavior depending on α [8]. Table 2 shows kinetic obedience and the Arrhenius parameters determined for the dehydration of the powdered materials of various particle-size fractions. We see from Table 2 that the initial and main stages of the reaction of crushed crystals of $-170+200$ and $-100+170$ mesh fractions are regulated by an A_m law, in contrast with the isothermal result. In addition, the two-dimensional diffusion-controlled (D_2) law, $\alpha+(1-\alpha)\ln(1-\alpha)=kt$, obeyed the later stage. As for the crushed crystals of $-48+100$ mesh fraction, it is very likely that the overall reaction is described by a D_L law. It is interesting that this is in agreement with the nonisothermal dehydration of the single crystal [1].

2. DSC

Figure 6 shows typical DSC curves and α vs. T plots obtained by integrating the DSC curves at various β [2]. The integrated curves were analyzed according to the Ozawa method. The E values thus estimated at various α were shown in Fig. 5. Such E values obtained from the DSC curves, as well as those from TG, also decrease as reaction advances. Table 3 shows kinetic obedience and the Arrhenius parameters determined within different limited ranges of α. We see from Fig. 5 and Table 3 that the E values determined from the integrated DSC curves increase with decreasing

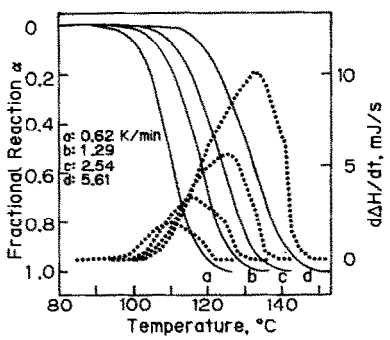

Fig. 6. Typical DSC curves, and plots of α vs. T obtained by integrating the DSC curves.

TABLE 3

The most appropriate kinetic rate function, $F(\alpha)$, and Arrhenius parameters, E and log A, determined by the Ozawa method from the integrated DSC curves of the nonisothermal dehydration of crushed crystals of different particle-size fractions within various α ranges

Range of α	Particle-size fraction (mesh)											
	−170+200				−100+170				−48+100			
	$F(\alpha)$	E(kJ mol^{-1})	log A (s^{-1})	r [a]	$F(\alpha)$	E(kJ mol^{-1})	log A (s^{-1})	r [a]	$F(\alpha)$	E(kJ mol^{-1})	log A (s^{-1})	r [a]
0.1–0.9	$A_{1.2}$	138±4	15.9±0.5	0.9996	$A_{1.2}$	126±3	14.2±0.4	0.9997	$A_{1.1}$	125±3	14.1±0.4	0.9981
0.1–0.5	$A_{1.0}$	151±5	17.5±0.6	0.9999	$A_{1.2}$	132±4	15.0±0.4	0.9989	$A_{1.1}$	138±4	15.9±0.5	0.9999
0.2–0.6	$A_{1.1}$	140±4	16.2±0.5	0.9999	$A_{1.3}$	127±3	14.3±0.4	0.9996	$A_{1.1}$	129±3	14.7±0.4	0.9998
0.3–0.7	$A_{1.1}$	134±4	15.3±0.4	0.9999	$A_{1.3}$	124±3	13.9±0.4	0.9996	$A_{1.2}$	122±3	13.7±0.3	0.9999
0.4–0.8	$A_{1.2}$	129±3	14.6±0.4	0.9999	$A_{1.0}$	122±3	13.7±0.4	0.9996	$A_{1.2}$	116±2	12.9±0.2	0.9999
0.5–0.9	$A_{1.8}$	125±3	14.0±0.4	0.9994	$A_{1.3}$	120±2	13.4±0.4	0.9995	$A_{1.1}$	110±2	12.2±0.2	0.9999

[a] Correlation coefficient of the linear regression analysis of the $F(\alpha)$ vs. θ plot.

particle size. This seems to be due to the kinetic compensation behavior, because the variation in E is accompanied by the parallel change in log A [9]. It is noted, at the same time, that the kinetic laws are different between the TG and DSC analyses, particularly for larger particle-size fractions and at later stages of dehydration. This is ascribed to the fact that TG and DSC respond to a mass-loss of water vapor from the system and a total enthalpy change due to dehydration including exothermic crystallization of the solid product, respectively. In other words, TG curves are sensitive to diffusion and desorption of water vapor through and out of the solid phase. DSC curves are largely influenced by the extent and rate of crystallization of the solid product. This explains the fact that, with the sample of a $-48 + 100$ mesh sieve fraction, dehydration obeys, according to the TG and DSC analyses, one of the diffusion-controlled laws, $D_L = kt$, and Avrami–Erofeyev laws, $A_m = kt$, respectively. It is rather difficult to interpret the meaning of the exponents of m and L in these laws on a theoretical basis, because small particles were used and averaging of the actual processes over the many particles is taking place.

Kinetic comparison between the isothermal and nonisothermal reactions

As described above, the isothermal dehydration of all the particle-size fractions obeyed an R_n law with $n \approx 1.4$. On the other hand, different kinetic obedience was observed among different particle-size fractions from nonisothermal TG analyses. Namely, the dehydrations of the smaller and larger particle-size fractions were regulated, as a whole, by laws of A_m and D_2, respectively (see Table 2).

Variation in kinetic obedience depending on the heating condition and on the particle size might be explained as follows. The isothermal dehydration initially proceeds through superficial nucleation and its growth, which then advances inwards. Under dynamic conditions, distribution of the α value at a given time among particles in a pan is larger than that under the isothermal condition [2]. Time lags in reaction occurring in many particles in a pan seem to be responsible for obedience to the A_m law derived from nonisothermal TG and DSC for the smaller particle-size fractions.

As for the larger particle sizes, the advancement of the reaction front following the surface reaction is regulated by phase boundary reaction and diffusion of water vapor through the solid product under isothermal and nonisothermal conditions, respectively. The above trend could be explained if the increase in the rate of advance of the reaction interface, caused by change in the heating condition from isothermal to dynamic, is much more marked than the corresponding increase in the rate of diffusion of the water vapor through the solid product. Another factor could be that more rapid crystallization of the product at the higher reaction temperatures impedes the escape of water vapor through the product phase [1,10–12]. This is

supported by the fact that the enthalpy change ΔH of the dehydration, obtained from the DSC curves, decreases gradually with increasing heating rate due to the more rapid crystallization, which is exothermic; $\Delta H = 53.3 \pm 0.8$ and 48.6 ± 0.8 kJ mol^{-1} at heating rates of 0.6 and 5.2 K min^{-1}, respectively.

ACKNOWLEDGEMENT

The authors wish to thank K. Oh-ike and C. Akaza for their assistance in the experimental part of this work.

REFERENCES

1 N. Koga and H. Tanaka, Thermochim. Acta, to be submitted.
2 H. Tanaka and N. Koga, Thermochim. Acta, 163 (1990) 295.
3 H. Tanaka and N. Koga, J. Therm. Anal., submitted.
4 T. Ozawa, Bull. Chem. Soc. Jpn., 38 (1965) 1881.
5 T. Ozawa, J. Therm. Anal., 2 (1970) 301.
6 T. Ozawa, Thermochim. Acta, 100 (1986) 109.
7 N. Koga and H. Tanaka, J. Therm. Anal., 34 (1988) 177.
8 N. Koga and H. Tanaka, J. Phys. Chem., 93 (1989) 7793.
9 H. Tanaka and N. Koga, J. Therm. Anal., 34 (1988) 685.
10 G.G.T. Guarini and M. Rustici, J. Therm. Anal., 34 (1988) 487.
11 G.G.T. Guarini and A. Magnani, React. Solids, 6 (1988) 277.
12 H. Tanaka and N. Koga, J. Phys. Chem., 92 (1988) 7023.